



THE UNIVERSITY *of* EDINBURGH

Edinburgh Research Explorer

Mixed-species RNA-seq for elucidating non-cell-autonomous control of gene transcription

Citation for published version:

Qiu, J, Dando, O, Baxter, P, Hasel, P, Heron, S, Simpson, T & Hardingham, G 2018, 'Mixed-species RNA-seq for elucidating non-cell-autonomous control of gene transcription' Nature Protocols. DOI: 10.1038/s41596-018-0029-2

Digital Object Identifier (DOI):

[10.1038/s41596-018-0029-2](https://doi.org/10.1038/s41596-018-0029-2)

Link:

[Link to publication record in Edinburgh Research Explorer](#)

Document Version:

Other version

Published In:

Nature Protocols

General rights

Copyright for the publications made accessible via the Edinburgh Research Explorer is retained by the author(s) and / or other copyright owners and it is a condition of accessing these publications that users recognise and abide by the legal requirements associated with these rights.

Take down policy

The University of Edinburgh has made every reasonable effort to ensure that Edinburgh Research Explorer content complies with UK legislation. If you believe that the public display of this file breaches copyright please contact openaccess@ed.ac.uk providing details, and we will remove access to the work immediately and investigate your claim.

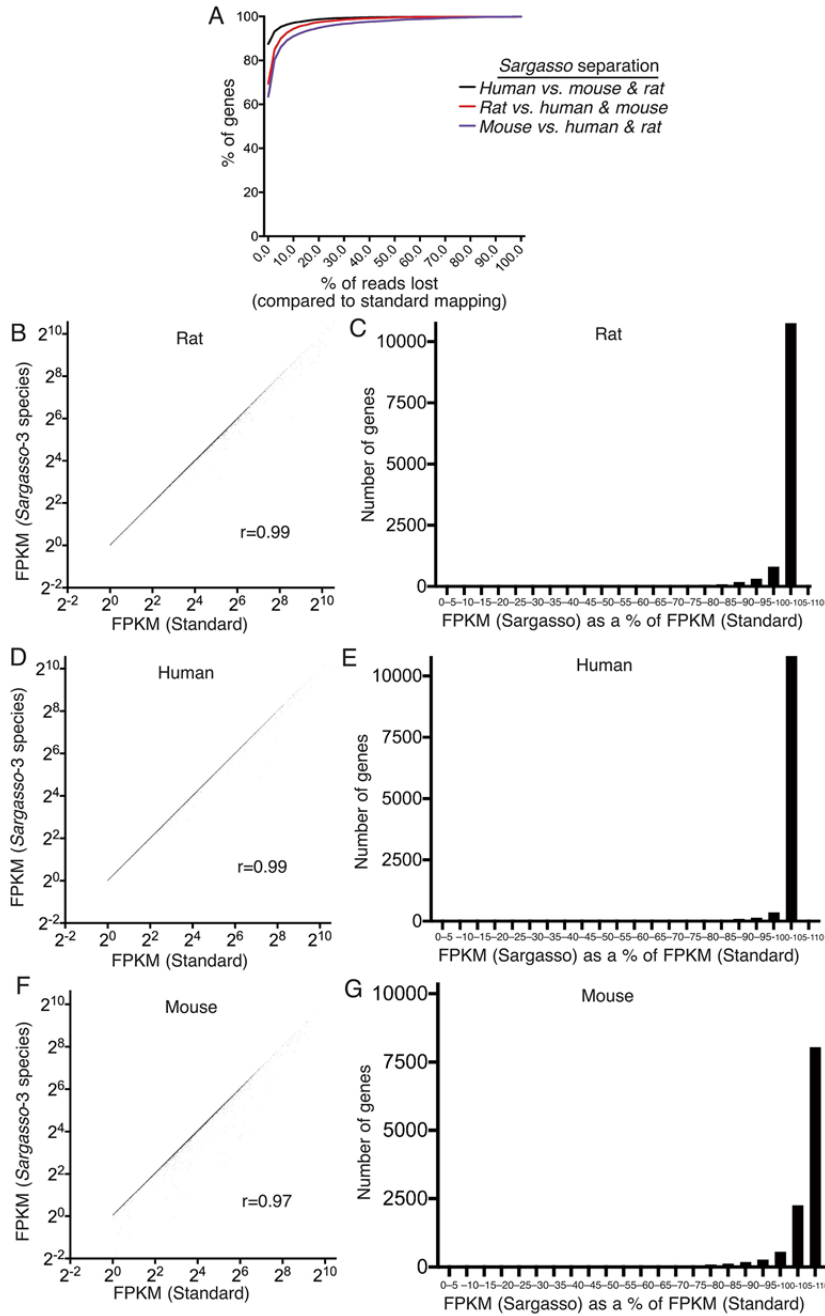


Supplemental Figures

Mixed-species RNA-seq for elucidating non-cell-autonomous control of gene transcription

Jing Qiu, Owen Dando, Paul Baxter, Philip Hasel, Samuel Heron, T. Ian Simpson, and Giles E. Hardingham

Supplementary Figure 1



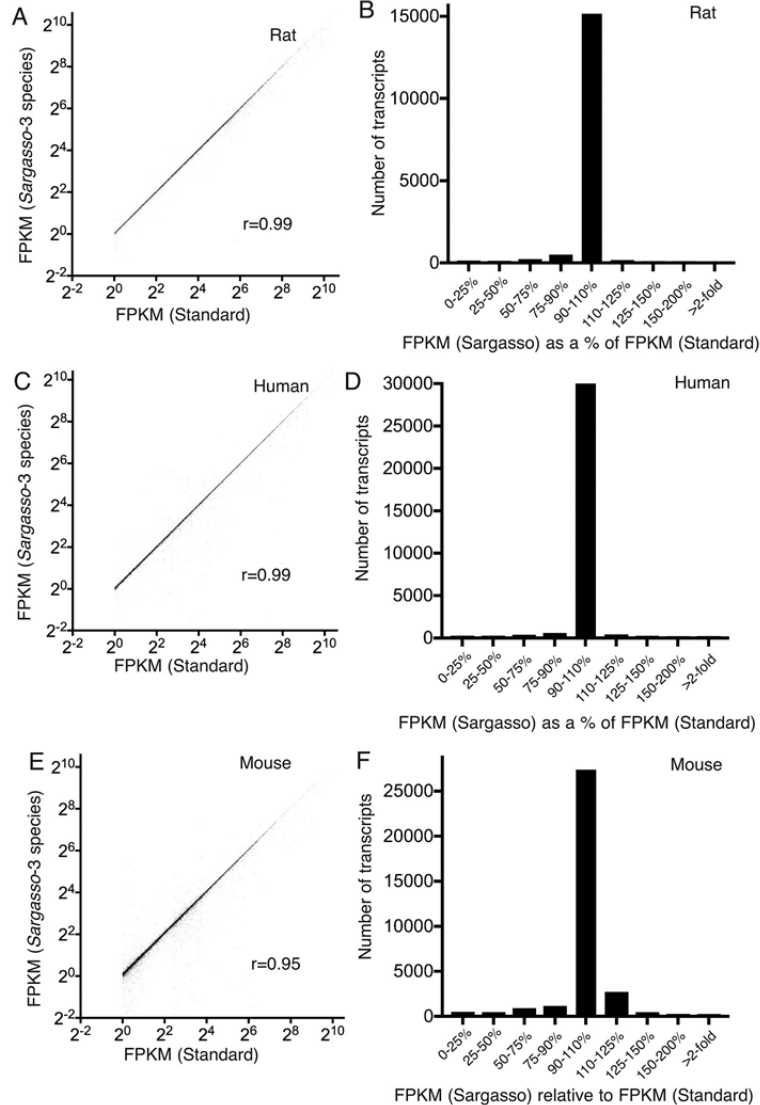
Supplementary Figure 1

Impact of *Sargasso* species disambiguation on gene expression quantification.

A) Single-species RNA-seq reads (rat samples MGLmonoCTR1–3 from ArrayExpress accession E-MTAB-5987 (this study), human samples GSM2285374–7 from Gene Expression Omnibus series GSE85839¹ and mouse samples CTR1-34316426, CTR2-34335325 and CTR3-34312414 from ArrayExpress accession E-MTAB-5489²), were taken, and we calculated the % reads lost for each protein-coding gene expressed >1 FPKM (by normal mapping—defined as mapping which requires perfect match to target species, but no disambiguation between any other species) when performing the *Sargasso* pipeline requiring disambiguation of reads from the other two species. A cumulative distribution plot for genes against % of reads lost is shown. **B,C)** For rat RNA-seq reads (rat samples MGLmonoCTR1–3 from E-MTAB-5987), gene FPKM values were calculated using normal mapping and *Sargasso* mapping,

requiring disambiguation of reads from mouse and human genomes. FPKM values were plotted against each other for all 12,432 protein-coding genes expressed >1 FPKM (by normal mapping) (B). In (C), the FPKM (*Sargasso*) was calculated as a % of the FPKM (normal mapping), and a frequency distribution of the genes shown (with 5% bin size). **D,E**) For human RNA-seq reads (samples GSM2285374–7 from GSE85839), gene FPKM values were calculated using normal mapping and *Sargasso* mapping, requiring disambiguation of reads from rat and mouse genomes. FPKM values were plotted against each other for all 11,668 protein-coding genes expressed >1 FPKM (by normal mapping) (D). In (E), the FPKM (*Sargasso*) was calculated as a % of the FPKM (normal mapping), and a frequency distribution of the genes shown (with 5% bin size). **F,G**) For mouse RNA-seq reads (mouse samples CTR1-34316426, CTR2-34335325 and CTR3-34312414 from E-MTAB-5489), gene FPKM values were calculated using normal mapping and *Sargasso* mapping, requiring disambiguation of reads from rat and human genomes. FPKM values were plotted against each other for all 11,971 protein-coding genes expressed >1 FPKM (by normal mapping) (F). In (G), the FPKM (*Sargasso*) was calculated as a % of the FPKM (normal mapping), and a frequency distribution of the genes shown (with 5% bin size).

Supplementary Figure 2



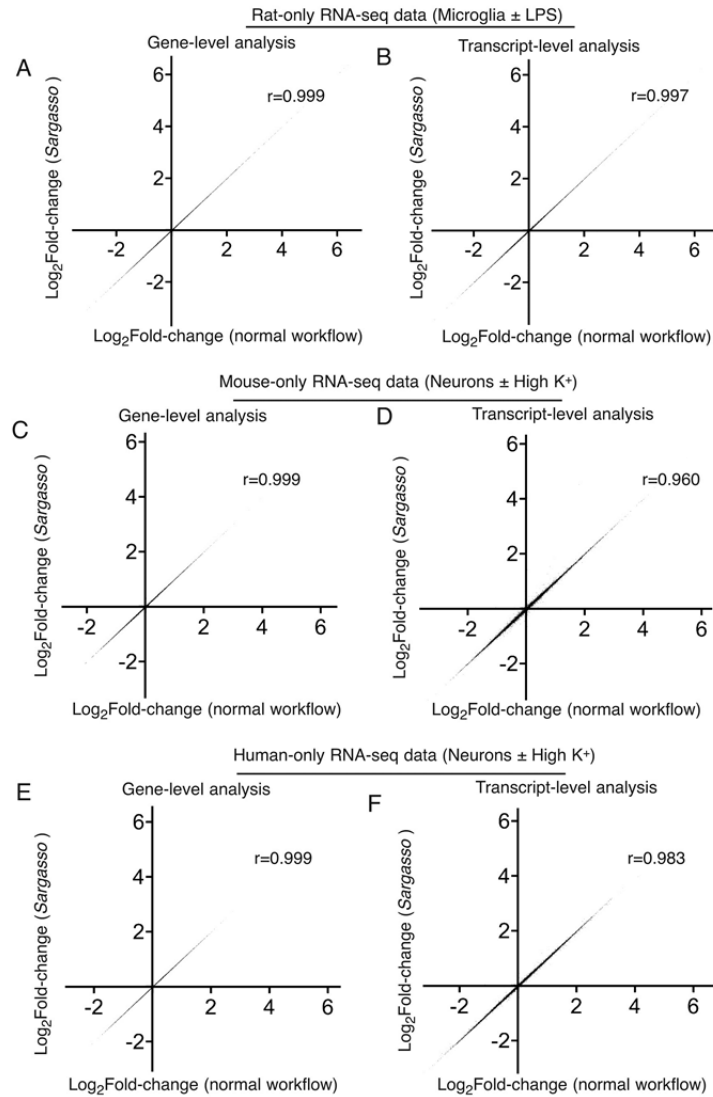
Supplementary Figure 2

Impact of the *Sargasso* species disambiguation on transcript expression quantification.

A,B) For rat RNA-seq reads (rat samples MGLmonoCTR1–3 from E-MTAB-5987), FPKM values of all transcripts of protein-coding genes (as annotated by Ensembl) were calculated using normal mapping and *Sargasso* mapping, requiring disambiguation of reads from mouse and human genomes. FPKM values were plotted against each other for all those 16,169 transcripts expressed >1 FPKM (by normal mapping) (A). In (B), the FPKM (*Sargasso*) was calculated as a % of the FPKM (normal mapping), and a frequency distribution of the transcripts shown. **C,D)** For human RNA-seq reads (samples GSM2285374–7 from GSE85839), FPKM values of all transcripts of protein-coding genes (as annotated by Ensembl) were calculated using normal mapping and *Sargasso* mapping, requiring disambiguation of reads from mouse and rat genomes. FPKM values were plotted against each other for all those 34,149 transcripts expressed >1 FPKM (by normal mapping) (C). In (D), the FPKM (*Sargasso*) was calculated as a % of the FPKM (normal mapping), and a frequency distribution of the transcripts shown. **E,F)** For mouse RNA-seq reads (mouse samples CTR1-34316426, CTR2-34335325 and CTR3-34312414 from E-MTAB-5489), FPKM values of all transcripts of protein-coding genes (as annotated by Ensembl) were calculated using normal mapping and *Sargasso* mapping, requiring disambiguation of reads from human and rat genomes. FPKM values were plotted against each other for all those 34,024 transcripts expressed >1 FPKM (by normal mapping) (E). In (F), the FPKM (*Sargasso*) was calculated as a % of the FPKM (normal mapping), and a frequency distribution of the transcripts

shown.

Supplementary Figure 3

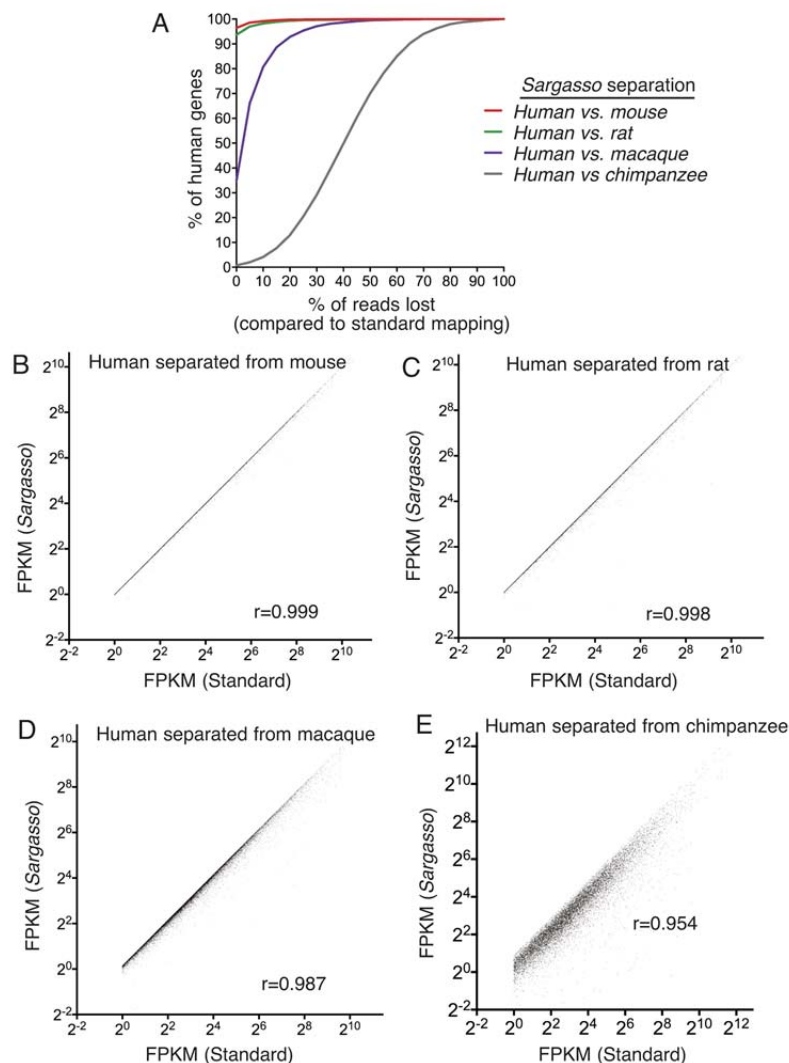


Supplementary Figure 3

Impact of *Sargasso* species disambiguation on stimulus-induced gene- and transcript- level fold induction quantification.

A,B) For rat RNA-seq reads (rat control samples MGLmonoCTR1–3, and LPS-treated samples MGLmonoLPS1–3, E-MTAB-5987 (this publication-sample sets 6a and 6b: see *Supplementary Results*), DESeq2 Log₂-fold change (LPS vs. Con) was calculated both at the gene level (A) and transcript level (B), using normal mapping, and for *Sargasso* mapping requiring disambiguation of reads from mouse and human genomes. For all genes/transcripts expressed > 1FPKM on average across the samples (by normal mapping), DESeq2 Log₂-fold change for the two approaches was plotted against each other, and a correlation coefficient calculated. **C,D)** For mouse RNA-seq reads (mouse DIV4 cortical neuron control samples, and high K⁺-treated samples, both from E-MTAB-5489²), DESeq2 Log₂-fold change (high K⁺ vs. Con) was calculated both at the gene level (C) and transcript level (D), using normal mapping, and for *Sargasso* mapping requiring disambiguation of reads from rat and human genomes. For all genes/transcripts expressed > 1FPKM on average across the samples (by normal mapping), DESeq2 Log₂-fold change for the two approaches was plotted against each other, and a correlation coefficient calculated. **E,F)** For human RNA-seq reads (human ES cell-derived neuron control samples, and high K⁺-treated samples, both from E-MTAB-5489²), DESeq2 Log₂-fold change (high K⁺ vs. Con) was calculated both at the gene level (E) and transcript level (F), using normal mapping, and for *Sargasso* mapping requiring disambiguation of reads from rat and mouse genomes. For all genes/transcripts expressed > 1FPKM on average across the samples (by normal mapping), DESeq2 Log₂-fold change for the two approaches was plotted against each other, and a correlation coefficient calculated.

Supplementary Figure 4

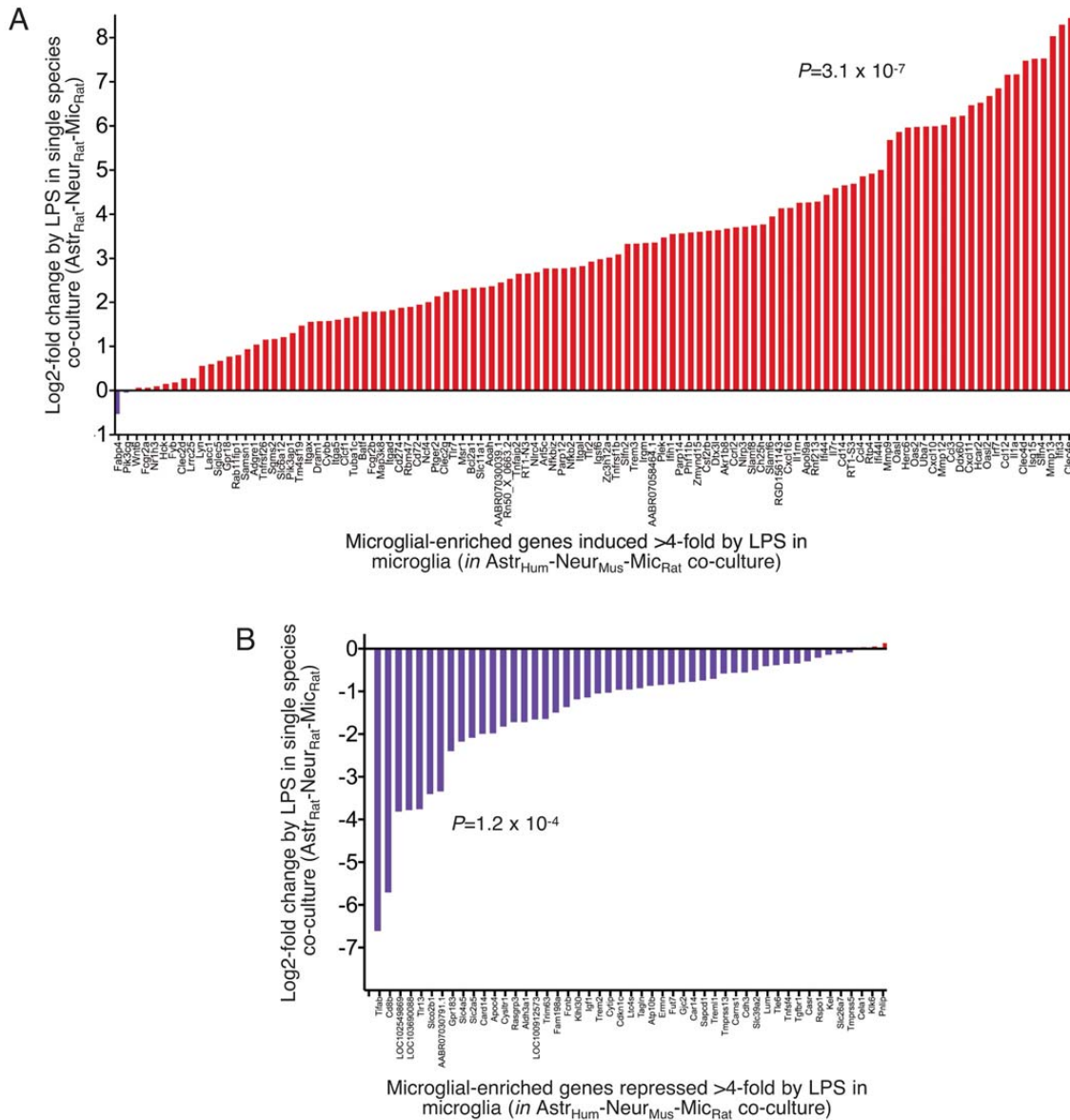


Supplementary Figure 4

Sargasso species disambiguation of human RNA-seq reads against species of varying evolutionary distance

A) Human RNA-seq reads (Gene Expression Omnibus samples GSM2285374–7¹), were taken, and we calculated the % reads lost for each protein-coding gene expressed >1 FPKM (by normal mapping – defined as mapping which requires perfect match to target species, but no disambiguation between any other species, 11,661 genes in total) when performing the *Sargasso* pipeline requiring disambiguation of reads against mouse, rat, macaque, or chimpanzee. A cumulative distribution plot for genes against % of reads lost is shown for each of the four *Sargasso* species disambiguation procedures. **B-E)** For the human RNA-seq reads in (A), FPKM values of all protein-coding genes were calculated using normal mapping and *Sargasso* mapping, requiring disambiguation of reads from mouse (B), rat (C), macaque (D) and chimpanzee (E). FPKM values were plotted against each other for all those 11,661 genes expressed >1 FPKM (by normal mapping), and the correlation coefficient calculated.

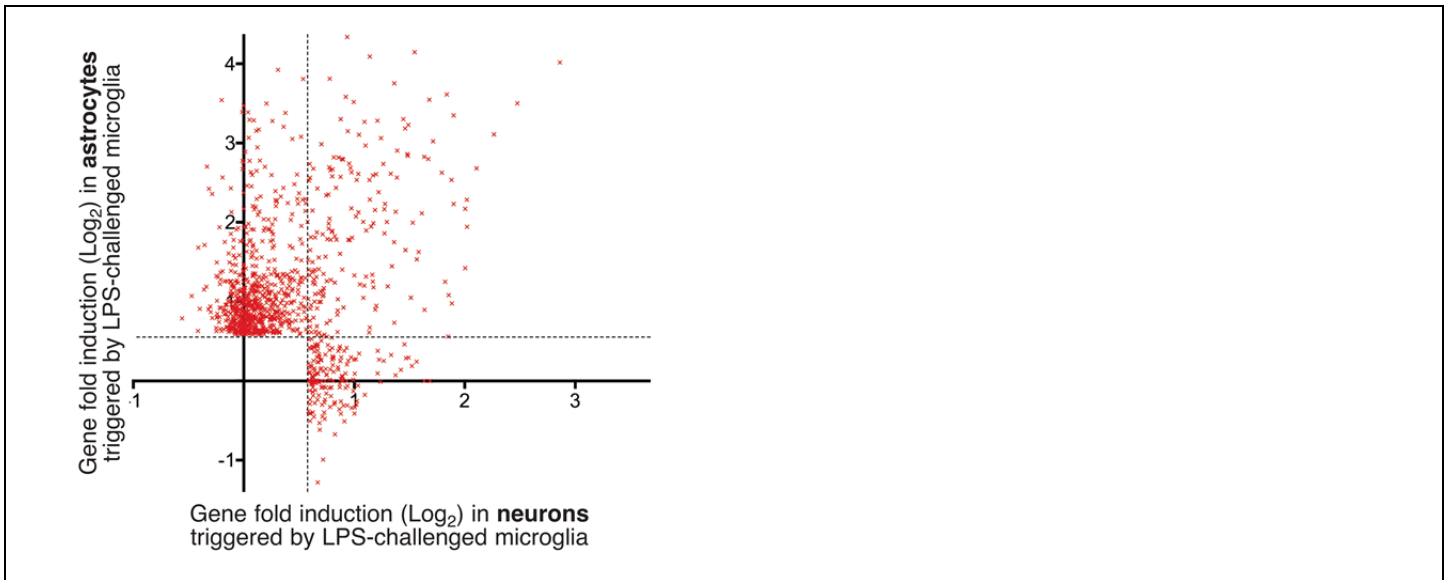
Supplementary Figure 5



Supplementary Figure 5

Expression changes induced by LPS in microglia are not influenced by having other cells present from different species.

A,B Differential gene expression analysis between samples 5a and 5b, co-cultures of rat microglia, neurons and astrocytes (\pm LPS). We took the list of genes significantly induced (304 genes) or repressed (113 genes) >4-fold by LPS treatment in rat microglia in the mixed species co-culture (samples 2a vs. 2b) and then looked at the LPS-dependent regulation of the subset of these genes whose induction could be tracked in a single species co-culture (5a vs. 5b) by virtue of their expression being >5-fold higher in a pure microglial culture, than the mixed microglia-astrocyte-neuron co-culture (samples 5a vs. 6a), and expressed at least 1 FPKM in mono-cultured microglia. Applying these criteria meant that we could, to a first approximation, monitor the regulation of 108/304 LPS-induced genes (A), and 44/113 LPS-repressed genes (B), in microglia in a single species microglia-neuron-astrocyte co-culture. The DESeq2 Log₂fold-change is shown for each of the 108 LPS-induced genes (A) and 44 LPS-repressed genes (B), and a *P* value calculated (paired t-test, samples 5a vs. 5b, $n=108$ (A), $n=44$ (B)).



Supplementary Figure 6

Activated microglia induce largely distinct specific transcriptional responses in neurons and astrocytes

For genes induced (>1.5-fold) by microglia in astrocytes (Fig. 2d) and in neurons (Fig. 2f), the fold change in neurons is plotted against that in astrocytes. The top-right quadrant formed by the crossed dotted lines includes those genes induced >1.5-fold by microglia in both neurons and astrocytes, a relatively small number of genes.

References

- 1 Muffat, J. *et al.* Efficient derivation of microglia-like cells from human pluripotent stem cells. *Nat Med* **22**, 1358-1367, doi:10.1038/nm.4189 (2016).
- 2 Qiu, J. *et al.* Evidence for evolutionary divergence of activity-dependent gene expression in developing neurons. *Elife* **5**, doi:10.7554/eLife.20337. e20337 [pii] (2016).